Korea Polymer Journal, Vol. 3, No. 2, pp 86-93 (1995)

Phase Separation Phenomena in Polystyrene Solutions

Seung-Won Song*

Yukong Taedok Institute of Technology

John M. Torkelson

Department of Chemical Engineering, Northwestern University
Evanston, Illinois 60208-3120, USA

Received August 1, 1995

ABSTRACT: The phase separation phenomena in polymer solutions were studied *via* phase diagrams of polystyrene-solvent systems determined by differential scanning calorimetry and turbidimetry method. It was demonstrated that the critical temperatures found in this study and the theta temperatures from the research literature, show a linear relationship as expected from the Shultz-Flory equation. Thermally induced phase separation (TIPS) process was employed to prepare microporous membranes, and the phase separation mechanisms were studied based on the phase diagram for the system. It has been shown that if polymer concentration is close to the critical point and phase separation is initiated in the unstable region, resulting in a spinodal decomposition mechanism, the membrane produced was well interconnected with highly uniform pore sizes and possesses mechanical strength. In contrast, the characteristic membrane morphology associated with polymer concentration being below the critical concentration and phase separation being initiated in the metastable region, resulting in a nucleation and growth mechanism, was a poorly interconnected, stringy and/or beady structure which is mechanically fragile.

Introduction

The principles of phase separation are central to an understanding of many scientific and technological disciplines, and are important guidelines in the production, processing and application of materials. Phase separation phenomena in polymer-solvent systems can be brought about by variations in temperature, pressure, and composition of the polymer solutions. Phase separation in polymer-solvent systems can be classified into two major categories: solid-liquid phase separation and liquid-liquid phase separation.[1] Solid-liquid phase separation results from vitrification or crystallization of one or all of the chemically different equilibrium liquid phases, and liquid-liquid phase separation results from the thermodynamic instability of a polymer-solvent system. While the mechanism of solid-liquid phase separation is generally the classic one of nucleation and growth, for liquid-liquid phase separation the mechanism depends on the state of the thermodynamic stability of the system. In one region, nucleation and growth predominates; in another, spinodal decomposition is the phase separation mechanism. Phase diagrams are concise plots of equilibrium relationships in heterogneous materials and are key to understand the phase separation mechanism.

Liquid-Liquid Phase Separation. The thermodynamic criteria for solubility in a two component polymer-solvent system can be expressed in terms of the Gibbs free energy of mixing, ΔG_m, and its second derivative with respect to polymer volume fraction, ϕ, at a fixed temperature T and pressure P[2,3]:

$$\Delta G_m < 0 \tag{1}$$

$$\left(\frac{\partial^2 \Delta G_m}{\partial \phi^2}\right)_{T,P} > 0 \tag{2}$$

If either criterion is not met, the solution may separate into two phases in equilibrium. As shown in Figure 1, when the locus of minima, for which the chemical potentials of each component are equal in both phases, is plotted in the form of a temperature-composition phase diagram, the resulting curve is referred to as the binodal. The limit of metastability, where $\partial^2 \Delta G_m / \partial \phi^2 = 0$, is called the

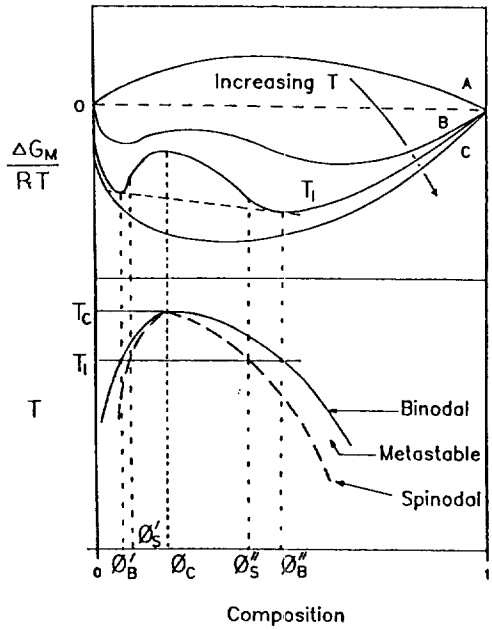

Figure 1. Gibbs free energy of mixing as a function of polymer volume fraction showing partial miscibility. Note minima ϕ_B' and ϕ_B'' of common tangent, inflection points ϕ_S' and ϕ_S'', critical point ϕ_C, and influence of temperature for a system possessing an upper critical solution temperature (UCST).

spinodal. Inside the spinodal, separation takes place by a continuous and spontaneous procedure occurring by a diffusional flux against a concentration gradient (uphill diffusion, i.e., the second derivative of Gibbs free energy of mixing, $\partial^2\Delta G_m/\partial\phi^2$, is negative).

In the unstable region, any small fluctuations in composition will lower the free energy and continue to grow. This procedure is called spinodal decomposition.[4] In the metastable region (the second derivative of Gibbs free energy of mixing is greater than zero) small fluctuations tend to decay, and hence phase separation can only proceed by overcoming a barrier with a large composition fluctuation. The process requiring an increase in the free energy to form initial fragments (nuclei) is referred to as nucleation. After a nucleus reaches a critical size, the system decomposes from the homogeneous region into the heterogeneous region with a decrease in free energy, and the nuclei grow in extent without changing composition, which is termed growth. This phase separation mechanism is called nucleation and growth.[5]

Phase Diagrams of Polymer Solution Systems. The phase diagrams of polymer soutions including binodal and spinodal curves can be determined by various experimental methods. Most studies have used light scattering techniques to determine the binodal or spinodal curves.[6-8] Light scattering can be used to determine the temperature dependence of the angular distribution of scattered intensity due to the local concetration fluctuations near the critical point. Turbidimetry methods have been utilized to determine phase equilibria of various polymer solutions.[9,10] By using a centrifugal apparatus, the coexistence curves of polystyrene in methyl cyclohexane have been measured.[11] (Chu *et al.* used a synchronous pulsed light to observe the phase transition, and they took advantage of the presence of centrifugal acceleration which permits the formation of the boundary between the two phases of a fluid system after phase separation).

Differential scanning calorimetry has also been a useful tool to study liquid-liquid phase separation.[12-14] In some polymer solution systems, the heat of demixing peak can be detected by commercially available differential scanning calorimeters (e.g. Perkin-Elmer). Even though the calorimetric analysis may not be as accurate as optical methods, the results for locating the demixing curve are comparable.[15] With a differential refractometer, the concentration of the two coexisting phases can be determined by measuring the refractive index for the solution and the pure solvent in each phase of the two coexisting phases.[16] Pulsed-NMR (nuclear magnetic resonance) has also been used to determine binodal compositions by capitalizing on the differences in relaxation times for the same nuclei in different phases.[17] Equilibrium phase diagrams of polymer-solvent systems also have been calculated using Flory-Huggins solution thermodynamics.[18,19]

Preparation of Membranes Based on Phase Diagrams. Liquid-liquid phase separation in polymer solutions has been used for many years in the preparation of microporous materials.[20] Polymeric membranes have been also a noble means to study the thermodynamics of phase separation in polymer solutions.[21-24] The characteristic morphology of the phase-separating polymer solutions resulting from a nucleation and growth mechanism is either a poorly interconnected, stringy, beady structure which is mechanically fragile or a well interconnected structure with highly nonuniform pore sizes.[25,26] The nucleation and growth mecha-

nism occurs in the metastable region. In contrast, spinodal decomposition occurring in the unstable region results in a well interconnected, mechanically strong struture with highly uniform pore sizes.

Experimental

Materials. Atactic, monodisperse polystyrene (PS) standards (Pressure Chemical) were used. PS was chosen because of the extensive characterization data available. PS is available commercially in a wide range of molecular weights, and even high-molecular weight PS can be obtained with a narrow molecular weight distribution.

Various PS-solvent systems including *isopycnic* (isodensity) PS-diethyl malonate systems, low-viscosity PS-cyclohexane systems, high-viscosity PS-diisodecyl phthalate systems were chosen. PS and diethyl malonate have matched densities ($\Delta\rho<0.002$ g/cm^3 at 25 ℃), and at room temperature (slightly below the binodal curve) solutions undergoing phase separation do not show any macroscopic phase separation effects until after 3 days. The organic chemicals were obtained in reagent grade from Aldrich (diisodecyl phthalate was obtained from TCI America) and used without further purification.

Construction of Phase Diagrams. Thermal analysis of the polymer solutions was carried out with a differential scanning calorimeter (Perkin-Elmer DSC-7). The binodal curve was determined from the onset temperature of the heat of demixing peak. Approximately 10 mg of polymer solution was placed into an aluminum pan and hermetically sealed. The sample was then scanned at cooling rates ranging from 1 to 40 ℃/min. A dry-ice/methanol mixture was used as the cooling medium. The initial temperature of polymer solution for the thermal analysis was well above the expected cloud point, and the solution was allowed to remain at that temperature for 5 min to ensure that it was homogeneous.

Turbidimetry measurements were also employed to determine the binodal points. An IBM 9410 UV-visible spectrophotometer was used as a turbidmeter in this study. Initially homogeneous solution is cooled at a sufficiently low rate (such as 0.3 ℃/min) until a sharp increase in optical density is observed. A transmission wavelength of 800 nm, not absorbed by the polymer soution, is used to follow turbidity.

Results and Discussions

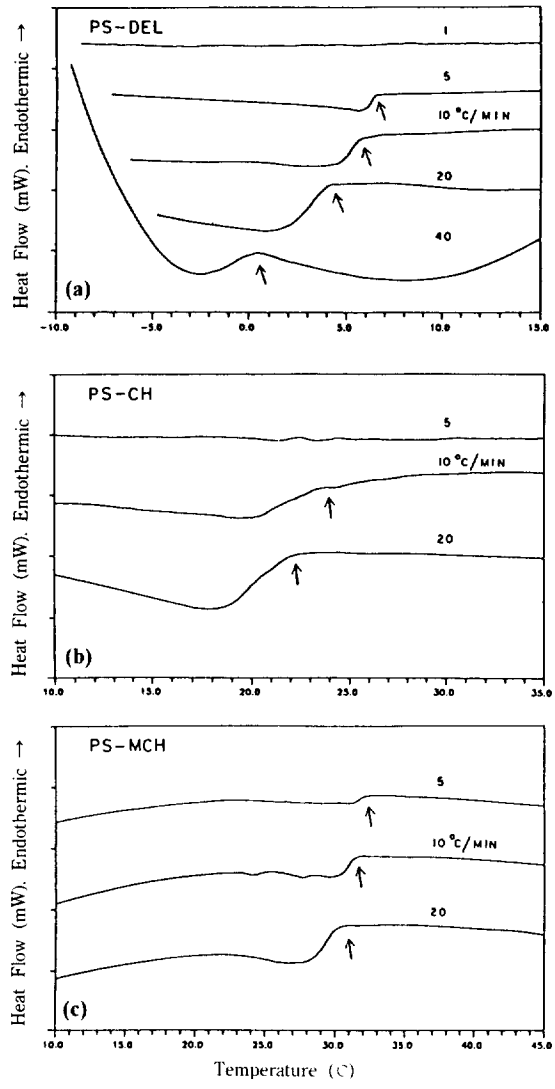

Figure 2. Differential scanning calorimetry of PS-solvent systems at different cooling rates: (a) 15 wt% PS-Decalin solution ($M_w=2.9\times10^5$); (b) 15 wt% PS-cyclohexane solution ($M_w=2.9\times10^5$); 13 wt% PS-methyl cyclohexane solution ($M_w=3.5\times10^4$).

Phase Diagrams. Figure 2 shows typical thermograms for various PS-solvent systems. The onst temperatures of the demixing peak are plotted as a function of a cooling rate showing a significant variation of the onset temperature associated with the heat of demixing as a function of cooling rate at a given concentration. The onset temperature obtained from the extrapolation of the cooling rate to 0 ℃/min was taken as the binodal point for the

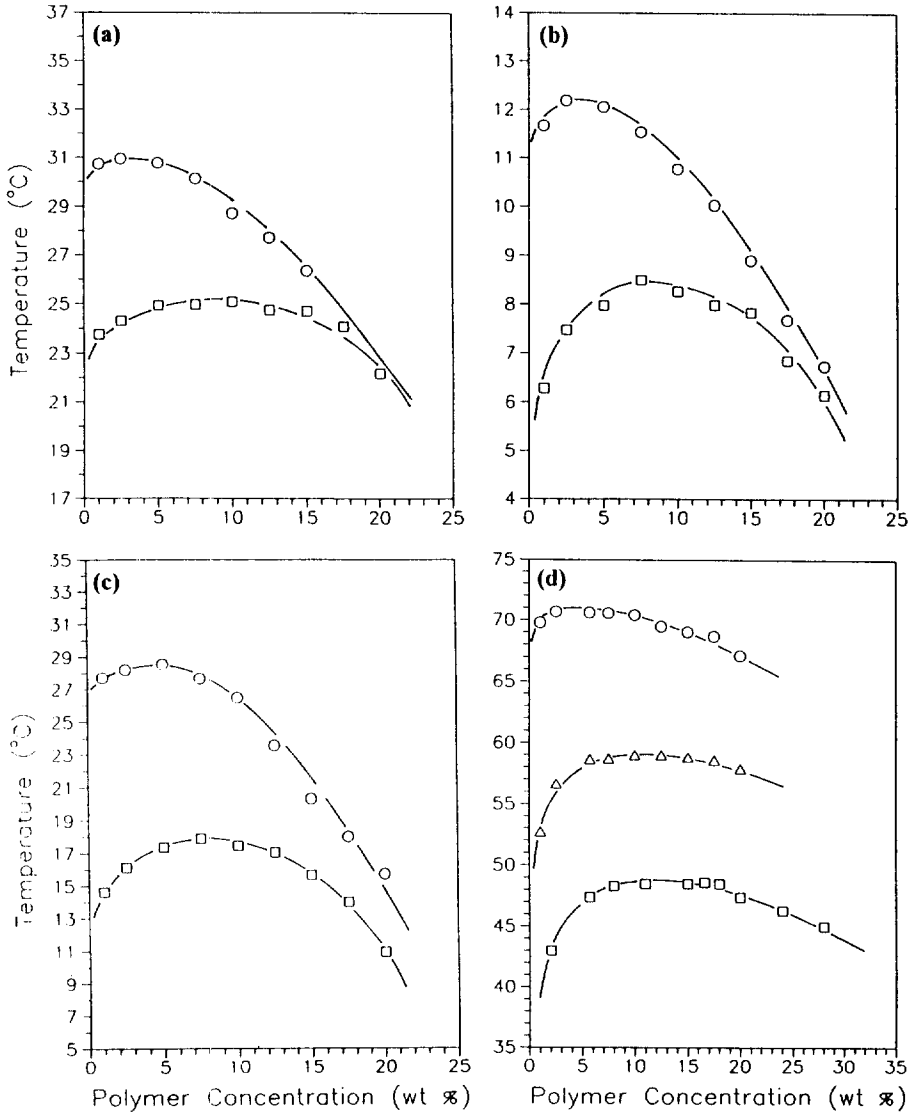

Figure 3. Cloud point curves for PS-solvent systems: (a) PS-cyclohexane; (b) PS-Decalin; (c) PS-diethyl malonate; (d) PS-diisodecyl phthalate: ( ) $M_w = 1.9 \times 10^6$; ( ) $M_w = 2.9 \times 10^5$; (■) $M_w = 1.1 \times 10^5$ Data replotted from the reference [S. Nojima, K. Shiroshita, and T. Nose, *Polymer J.*, **14**, 289 (1982)].

polymer solution. For a monodisperse polymer sample dissolved in a single solvent (hence a binary system), the cloud point curve coincides with the binodal. The threshold cloud point (the maximum of the cloud point curve) is the critical point. These features do not hold for solutions of polydispersed polymers.[23]

It should be noted that the use of differential scanning calorimetry was not successful for some polymer-solvent sysems employed in this study, such as PS-diethyl malonate and PS-diisodecyl phthalate, in attempts to determine the cloud point curve. In these systems, the demixing peaks were too small to be detected by Perkin-Elmer DSC-7 calorimeter for low polymer concentrations (such as 1 wt%). For the higher concentrations the peaks were often too broad to distinguish them from the base lines (in some cases, it is very difficult to tell whether the peak is very small or very broad). However, for the systems of PS-cyclohexane, PS-me-

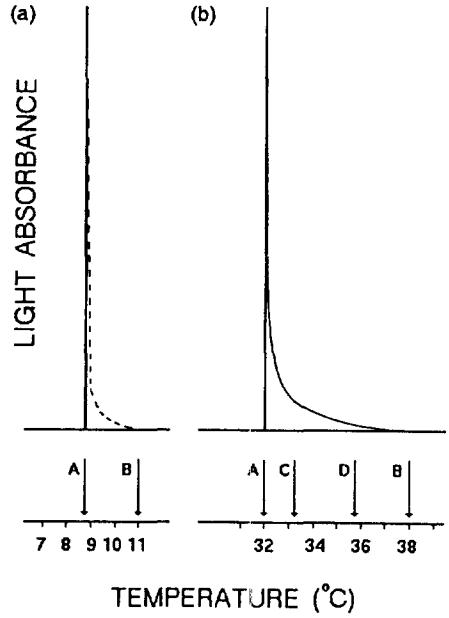

Figure 4. Determination of cloud points in polymer soutions by various measurements. Solid curve (a) denotes the light-absorbance of a PS-methyl cyclohexane solution, and dotted curve (b) denotes a light-absorbance of a PS-cyclohexane solution: (A) peak temperatures of light-absorbance; (B) onset temperatures of light-absorbance peak; (C) cloud point determined by thermal analysis (Figure 2); (D) cloud point determined by a refractive index measurement.[16]

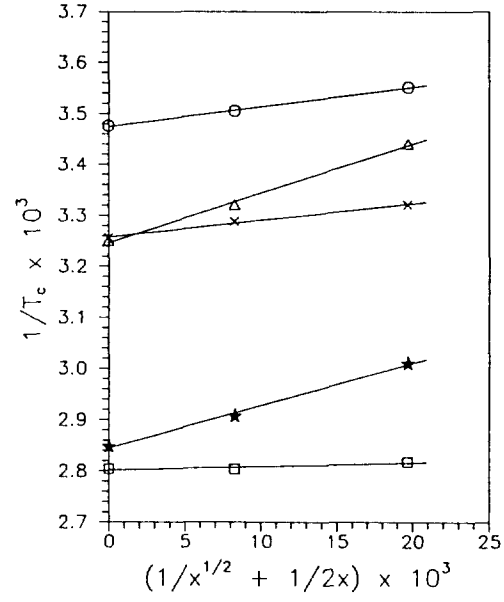

Figure 5. Dependence of critical temperature for phase separation on the value of $(1/x^{1/2}+1/2x)$ where x is the number of segments in polymer chain: (○) PS-Decalin; (△) PS-diethyl malonate; (×) PS-cyclohexane; (★) PS-diisodecyl phthalate; (□) PS-cyclohexanol.

thyl cyclohexane, and PS-Decalin, differential scanning calorimetry has been successful in determining the onset temperatures for phase separation. Figure 3 shows the phase diagrams of PS-solvent systems. The phase diagrams of PS-cyclohexane and PS-Decalin systems were determined by differential scanning calorimetry and those of PS-diethly malonate and PS-diisodecyl phthalate systems were determined by turbidmetry.

Figure 4 shows the cloud points of PS-solvent systems determined by various measurements. A refractive index measurement was done by Dobashi *et al.*[16] employing a 13 wt% of PS-methyl cyclohexane solution. Even though the M_w of PS ($M_w=3.5\times10^4$) used in the refractive index measurement is slightly different from the M_w of PS ($M_w=3.1\times10^4$) used in differential scanning calorimetry/turbidimetry measurements, the cloud points determined by these three measurements are comparable.

From Figure 4, it should be noted that a thermal analysis employing differential scanning calorimetry provides more clear information about the cloud point temperature than turbidimetry. A relatively wide range between onset and peak temperatures in light-absorbance curves often makes it difficult to determine an exact cloud point, even though the cloud point temperature is usually defined as the cross point of extrapolated base line and extrapolated peak line.

Critical Temperatures of Polymer-Solvent Systems. Shultz and Flory[27] derived the relationship between critical temperature, T_c, and the molecular weight of polymer,

$$\frac{1}{T_c}=\frac{1}{T_0}\left[1+\frac{1}{\psi_1}\left(\frac{1}{x^{1/2}}+\frac{1}{2x}\right)\right] \tag{3}$$

where ψ_1 is the entropy parameter and x is the number of repeat unit per polymer chain. Thus $1/T_c$ (K) varies linearly with $(1/x^{1/2}+1/2x)$, which is very nearly $1/x^{1/2}$ when x is large. The critical temperature is the highest temperature of phase separation. Theta (θ) temperatures can be obtained from the intercepts at $x=\infty$ in the plot of $1/T$ *vs.* $(1/x^{1/2}+1/2x)$. Determination of theta temperature by the extrapolation as described here is usually referred to

Table I. Physical Data of Solvents

Solvent	T_θ with PS (℃)	Viscosity at 25 ℃ (cp)
Cyclohexane	34.5	0.88
Decalin	14.5	1.68
Cyclohexanol	83.5	56.45
Diethyl malonate	35.8	2.35
Diisodecyl phthalate	79.0	81.45

as the Shultz-Flory method.

The theta temperature (T_θ or Flory temperature) is defined as a critical miscibility temperature in the limit of infinite molecular weight.[28] A solvent used at T_θ is called theta solvent, in which the free energies of solvent-solvent, solvent-polymer, and polymer-polymer interactions are all the same. (In a "poor" solvent the polymer would be expected to coil up so as to maximize the polymer-polymer interactions, while in a "good" solvent the polymer chain would tend to stretch out in order to maximize the polymer-solvent interactions). In principle, any solvent will become a theta-solvent for a given polymer at the theta temperature.[29]

Figure 5 shows the dependence of critical temperature (T_c) on the molecular weight for various solvent systems under study. The critical temperatures determined in this study and the theta temperatures from the research literature, show a linear relationship in Figure 5 as expected from equation (3). Note that in PS-diethyl malonate or PS-diisodecyl phthalate systems, a small change in molecular weight can result in a big difference in critical temperatures as shown in Figure 5. Table 1 shows theta temperatures of various solvents with PS, and solvent viscosities.[30]

Application of Phase Diagrams in Membrane Preparation. In the thermally induced phase separation (TIPS) process, the morphology of membranes prepared at short phase separation times from a two-component polymer-solvent system can be understood from the phase diagram for the system.[31] Figure 6 shows the phase diagram and two membranes produced from a 2.9×10^5 M_w PS-cyclohexanol system. The cloud point curve was determined experimentally using turbidimetry while the spinodal curve was approximated based on calculations employing information from the cloud point curve.[32] With this relatively flat cloud point curve, the critical concentration may be approximated as 10 wt% PS and the critical temperature as 81.8 ℃ (± 0.2 ℃). For the PS-cyclohexanol system, cloud point data were taken for another molecular weight

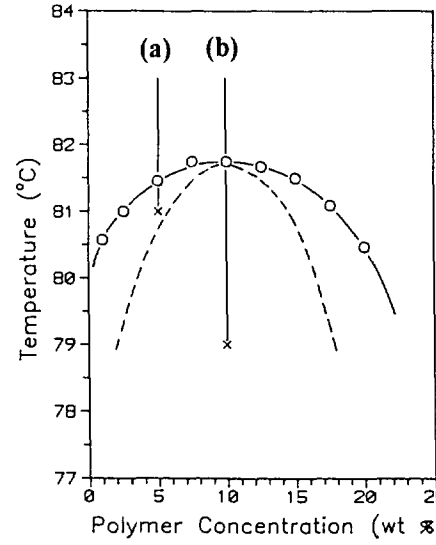

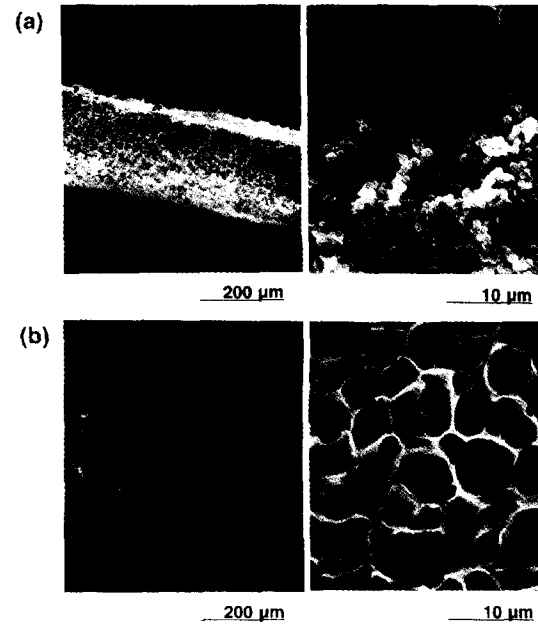

Figure 6. Scanning electron micrographs of the cross section of PS membranes with different quench routes: (a) membrane was prepared by quenching a 5 wt% PS-cyclohexanol ($M_w=2.9\times10^5$) solution to 81 ℃ for 1 min prior to freeze-drying, (b) membrane was prepared by quenching a 10 wt% PS-cyclohexanol ($M_w=2.9\times10^5$) solution to 79 ℃ for 1 min prior to freeze drying. The cloud point curve was prepared from turbidimetry and the spinodal curve was calculated.

of PS (1.9×10^6 M_w), revealing little molecular weight dependence of the cloud point curves for the PS-cyclohexanol system (see Figure 5). The data obtained were consistent with an earlier study by Schulz and Baumann who indicated that the θ-temperature for the PS-cyclohexanol system was 83.5 ℃.[33]

In Figure 6(a), the membrane was made from a 5 wt% solution phase separated at 81 ℃ which according to the phase diagram is believed to be in the metastable region. The polymer solution was then fast-frozen in liquid N_2, and solvent removal occurred by freeze drying with a VirTis bench top freeze dryer. The resulting membrane was further dried overnight in a vacuum oven at about 40 ℃. In the metastable region, phase separation proceeds by a nucleation and growth mechanism. In this case, as the polymer concentration is below the critical concentration, it is expected that phase separation will proceed with nucleation of the polymer-rich phase. The cross-section of the membrane in Figure 6(a) reveals a morphology of weakly connected polymer beads which is consistent with expectations for a nucleation and growth phase separation mechanism. In Figure 6(b) the membrane was made from a 10 wt% solution phase separated at 79 ℃ in the unstable region of the phase diagram. In the unstable region, phase separation proceeds by spinodal decomposition, and the resultant morphology is expected to be highly interconnected with relatively uniform pore size. The scanning electron micrograph in Figure 6(b) reveals a morphology consistent with expectations.

As shown in Figure 6, the morphology of polymeric membranes prepared from a two-component polymer-solvent system can be expected from the phase diagram for the system. It has been shown that if polymer concentration is close to the critical point and phase separation is initiated in the unstable region, resulting in a spinodal decomposition mechanism, the membrane produced will be well interconnected with highly uniform pore sizes and possess mechanical strength. In contrast, the characteristic membane morphology associated with polymer concentration being below the critical concentration and phase separation being initiated in the metastable region, resulting in a nucleation and growth mechanism, will be a poorly interconnected, stringy and/or beady structure which is mechanically fragile.

References

(1) O. Olabisi, L. M. Robeson, and M. T. Shaw, *Polymer-Polymer Miscibility*, Academic Press, New York, NY, 1979.
(2) M. Kurata, *Thermodynamics of Polymer Solutions*, Trans. H. Fujita, Harwood Academic Publishers, Chur, Switzerland, 1982.
(3) K. Kamide, *Thermodynamics of Polymer Solutions: Phase Equilibria and Critical Phenomena*, Polymer Science Library, Vol. 9, Elsevier, Amsterdam, The Netherlands, 1990.
(4) J. W. Cahn, *Trans. AIME*, **242**, 166 (1968).
(5) L. P. McMaster, Chap. 5, in *Copolymers, Polyblends, and Composites, Advances in Chemistry Series*, no. 142., Ed. N. A. J. Platzer, American Chemical Society, Washington, DC., 1975.
(6) J. J. van Aartsen and C. A. Smolders, *Eur. Polym. J.*, **6**, 1105 (1970).
(7) R. Koningsveld, L. A. Kleintjens, and H. M. Schoffeleers, *Pure Appl. Chem.*, **39**, 1 (1974).
(8) B. Chu, *Laser Light Scattering: Basic Principles and Practice*, 2nd ed., Academic Press, Inc., Boston, MA, 1991.
(9) Y. C. Bae, S. M. Lambert, D. S. Soane, and J. M. Prausnitz, *Macromolecules*, **24**, 4403 (1991).
(10) S. S. Kim and D. R. Lloyd, *Polymer*, **33**, 1047 (1992).
(11) B. Chu, K. Linliu, P. Xie, Q. Ying, Z. Wang, and J. W. Shook, *Rev. Sci. Instrum.*, **62**, 2252 (1991).
(12) P. T. van Emmerik and C. A. Smolders, *Eur. Polym. J.*, **9**, 293 (1973).
(13) H. Janeczek, E. Turska, T. Szekely, M. Lengyel, and F. Till, *Polymer*, **19**, 85 (1978).
(14) E. Maderek and B. A. Wolf, *Polym. Bull.*, **10**, 458 (1983).
(15) P. Vandeweerdt, H. Berghmans, and Y. Tervoort, *Macromolecules*, **24**, 3547 (1991).
(16) T. Dobashi, M. Nakata, and M. Kaneko, *J. Chem. Phys.*, **72**, 6685 (1980).
(17) G. T. Caneba and D. S. Soong, *Macromolecules*, **19**, 369 (1986).
(18) W. R. Burghardt, *Macromolecules*, **22**, 2482 (1989).
(19) K. Kamide, H. Iijima, and S. Matsuda, *Polymer J.*, **25**, 1113 (1993).
(20) S.-W. Song, Ph.D. Dissertation, Northwestern Univ., Evanston, Illinois, 1994.
(21) F.-J. Tsai and J. M. Torkelson, *Macromolecules*, **23**, 775 (1990).
(22) F.-J. Tsai and J. M. Torkelson, *Macromolecules*, **23**, 4983 (1990).
(23) S.-W. Song and J. M. Torkelson, *Polymer Preprints*, **34**, 496 (1993).
(24) S.-W. Song and J. M. Torkelson, *Macromolecules*, **27**, 6389 (1994).
(25) R. M. Hikmet, S. Callister, and A. Keller, *Polymer*, **29**, 1378 (1988).
(26) S.-W. Song and J. M. Torkelson, *J. Membrane Sci.*, **98**, 209 (1995).
(27) A. R. Shultz and P. J. Flory, *J. Am. Chem. Soc.*, **74**, 4760 (1952).
(28) P. J. Flory, *Principles of Polymer Chemistry*, Cornell

University Press, Ithaca, NY, 1953.
(29) H. R. Allcock and F. W. Lampe, *Contemporary Polymer Chemistry*, Prentice-Hall, Englewood Cliffs, NJ, 1981.
(30) J. Brandrup and E. H. Immergut, eds., *Polymer Handbook*, 3rd ed., A Wiley-Interscience Publishing, John Wiley & Sons, New York, NY, 1988.
(31) R. M. Hikmet, S. Callister, and A. Keller, *Polymer*, **29**, 1378 (1988).
(32) R.-Q. Li, *Can. Met. Quart.*, **30**, 15 (1991).
(33) G. V. Schulz and H. Baumann, *Makromol. Chem.*, **60**, 120 (1963).